



## ELASTIC NO TENSILE RESISTANT – PLASTIC ANALYSIS OF MASONRY ARCH BRIDGES AS AN EXTENSION OF CASTIGLIANO’S METHOD

A. Brencich<sup>1</sup>, U. De Francesco<sup>2</sup>, L. Gambarotta<sup>3</sup>

### ABSTRACT

On the basis of the classical Castigliano’s theory, a step-wise procedure for the non-linear analysis of multi-span masonry arch bridges is developed and implemented by standard programming of a commercial F.E. code. The mechanical model for masonry is assumed perfectly elasto-plastic in compression and no tensile resistant (NTR). The iterative procedure is set following the standard scheme of an elastic prevision and subsequent non-linear correction of the nodal forces. Tensile stresses are not allowed to develop on the mortar joint by means of an adequate re-meshing of the arch, while the plastic response is taken into account via additional fictitious external forces.

The procedure is applied to a flat arch with different models: a No Tensile Resistant (NTR) model that accounts for the original Castigliano’s method, and models with different compressive strength. The structural response is estimated for different loading positions, pointing out the change of the collapse mechanism as a function of the geometric and mechanical parameters. The flexibility of the procedure allows the analysis of twin-span and three-span models, so that the effect of abutment compliance and material crushing in complete bridge models is taken into account and quantified.

**Key words:** arch collapse analysis; multi-span arch bridges; non-linear interface model; elasto-plastic mortar joints.

Common address:

Department of Structural and Geotechnical Engineering – University of Genoa - ITALY  
DISEG, via Montallegro 1 – 16145 Genova - ITALY

<sup>1</sup>brencich@diseg.unige.it <sup>2</sup>defrancesco@diseg.unige.it <sup>3</sup>gambarotta@diseg.unige.it

## INTRODUCTION

A large number of ancient arch bridges is still in service in their original configuration, facing increasing vehicle loads and speed; for this reason reliable estimates of the structural response of these bridges are needed.

The classical methods of assessment (Heyman, 1982) refer to a single arch, assuming that the skewbacks are perfect built-in ends and considering simplified loading conditions. These procedures do not give any estimate of the structural response but either ensure the existence of an equilibrium configuration or give rough estimates of the limit load. The parameters relevant to the structural response, such as masonry strength, mechanical characteristics of the fill, adjacent spans, etc., are taken into account by means of corrective factors (Department of Transport, 1993.a,b, Hughes and Blackler, 1997) of uncertain heuristic origin.

To get a deeper insight in this kind of structures several different procedures have been developed (Hughes and Blackler, 1997) on the basis of a relevant series of experimental tests both on models and on real structures (Page, 1987, 1993).

The mechanism approach to arch collapse, originated from the first work of Pippard and Ashby (1939) and Pippard (1948), looks for the minimum load, once its position is defined, needed to introduce a number of hinges at the arch intradoes and extradoes large enough to transform the arch into a mechanism. The limit load is obtained through an application of the kinematic theorem (Heyman, 1982) that takes the position of the hinges as the unknowns of the problem. This approach finds its latest results in the work by Criesfield and Packham (1988), Harvey (1988), Blasi and Foraboschi (1994), Falconer (1994), Gilbert and Melbourne (1994), Hughes (1995) and Como (1998).

Such an approach is suitable for semicircular arches provided that the mechanism activates when the stress state is still rather limited, but this is not so for flat arches or for arches with very weak mortar joints. In this case the compressive stresses turn out to be significantly high when a collapse mechanism is still far from activating, so that the non linear elasto-plastic response of masonry, i.e. of the mortar joints, becomes a relevant parameter of the structural behaviour of the arch.

The elasto-plastic collapse can be dealt with in several ways. On the basis of simplifying assumptions for the plastic stress distribution in the mortar joints (Clemente et al., 1995) or of experimental tests (Taylor and Mallinder, 1993, Boothby, 1997) yield surfaces are obtained following the classical approach to plasticity; the limit load is obtained assuming that collapse is met when the axial thrust and the bending moment from the thrust line theory lie on the limit surface.

Another popular method of assessment makes use of F.E. procedures. The local collapse condition is usually derived from experimental tests and introduced into a F.E. model in which the arch is considered a mono-dimensional structure (Criesfield, 1985, Bridle and Hughes, 1990, Choo et al., 1991, Molins and Roca, 1998.a,b) a bi-dimensional (Loo and Yang, 1991, Falconer, 1994, Boothby et al., 1998, Owen et al., 1998, Ng et al. 1999, Lourenço and Rots, 2000, among the latest results) or three-dimensional one (Rosson et al., 1998). While mono-dimensional models proved to be reliable and flexible enough to be used in assessment and design procedures for arch bridges, requiring limited

computational effort, bi- and three-dimensional models are able of giving detailed information on local phenomena at expenses of a relevant complexity of the model and of long computing times. For this reason analyses of multi-span arch bridges have been performed, up to present, mainly by means of mono-dimensional finite elements (Molins and Roca, 1998.b), while bi-dimensional analyses had to be limited to quite simple models (Falconer, 1994).

The effect of the adjacent spans on the loaded arch had also been studied experimentally on 1:5 multi-span bridge models (Royles and Hendry, 1991, Melbourne and Wagstaff, 1993, and Melbourne et al., 1995, Ponniah and Prentice, 1998) and of mechanism ones (Hughes, 1995). The results, neglecting the elasto-plastic response of the joints, show a reduction of the limit load due to the presence of the adjacent arches somewhere in-between 20% to 50% of the limit load for a single span arch bridge.

In this paper, following the approach by Bridle and Hughes (1990) and Choo et al. (1991), Castigliano's elastic method (1879) is implemented in a mono-dimensional F.E. procedure and is extended in order to take into account the plastic response of the mortar joints. The flexibility of the procedure allows the analysis of several single, twin and multi-span arch bridges pointing out the way the structural response of the bridge is affected by the different mechanical and geometrical factors, i.e. masonry strength and arch barrel geometry. The obtained results give further information on the arch collapse mechanisms, allowing some considerations on the multi-span arch bridge structural behaviour.

### ELASTO-PLASTIC EXTENSION OF CASTIGLIANO'S APPROACH

According to Castigliano's approach, the interface between adjacent voussoirs can be represented by means of an elastic unilateral contact surface. In this way no traction is allowed to develop on the interface and no limit is set to the compressive stresses developed in the joint, Fig. 1.

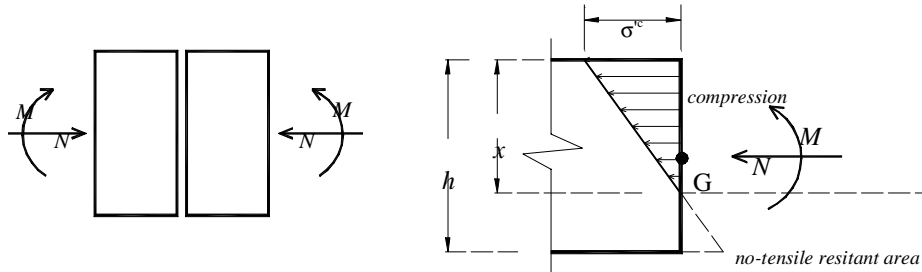


**Fig. 1.** No-tensile resistant model for the voussoirs' interface, Castigliano (1879)

The constitutive equations for the no-tensile resistant model can be derived in terms of the effective section height  $x$ :

$$N^E = \sigma_c \frac{bx}{2}, \quad M^E = \sigma_c \frac{bx}{2} \left( \frac{h}{2} - \frac{x}{3} \right) = N^E \left( \frac{h}{2} - \frac{x}{3} \right), \quad (1.a,b)$$

where the superscript  $E$  stands for the forces equilibrated by a No Tensile Resistant material fully elastic in compression.

In Castigliano's original work this model is assumed to represent dry assemblages of voussoirs or weak mortar joints. In the first case the model is somewhat questionable because it does not take into account the spalling collapse of the compressed edge (Taylor and Mallinder, 1993). On the other side mortar joints are subjected to a bi-axial compressive stress state due to the confinement effect of the voussoirs and, therefore, can exhibit quite high compressive stresses and significant plastic strains.

An improved mechanical model of the interface should assume a limit stress  $\sigma_c$  in compression beyond which plastic strains are allowed. Even though the proposed procedure is general and not related to a specific elasto-plastic model for the mortar joint, in the following reference is made to a perfect elasto-plastic constitutive model.

Under the plane section hypothesis, i.e. a linear distribution of strains, Fig. 2, the constitutive equations for the joints can be derived:

$$N^{EP} = \sigma_c \frac{b}{2}(x+y) \quad M^{EP} = \sigma_c \frac{b}{2} \left[ \frac{h}{2}(x+y) - \frac{1}{3}(x^2 + xy + y^2) \right] \quad (2.a,b)$$

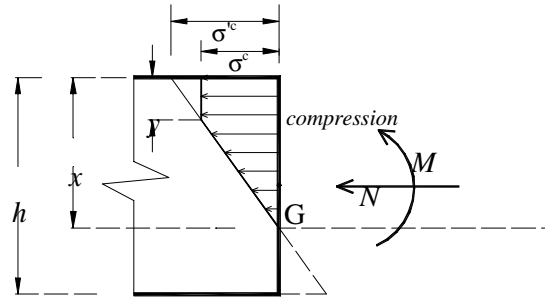


**Fig. 2.** No-tensile resistant perfect compressive elasto-plastic model for the joint interface.

The plastic cut-off of Fig. 2 can be computed as the difference between the elastic response of the effective section  $x$  – eq.s (1) – and the elasto-plastic response – eq.s (2):

$$\Delta N^{EP} = N^E - N^{EP} = \sigma_c \frac{b}{2} \frac{y^2}{x-y} \quad (3.a)$$

$$\Delta M_{EP} = M^E - M^{EP} = \sigma_c \frac{b}{2} \left[ \frac{h}{2} \frac{y^2}{x-y} - \frac{1}{3} \frac{y^3}{x-y} \right] = \Delta N^{EP} \frac{h}{2} - \sigma_c \frac{b}{6} \frac{y^3}{x-y} \quad (3.b)$$

The constitutive eq.s (2) and (3) are suitable for setting up an iterative procedure for the analysis of masonry arch-type structures. Even though this interface model has been developed with reference to a perfectly elasto-plastic response of the mortar joint but is suitable to represent also more complex constitutive models.

Consider an assemblage of voussoirs, such as the straight lintel of Fig. 3, with an axial thrust and bending moment high enough to induce opening at the bottom edge and to reach the limit compressive stress at top edge of the voussoirs, like in Fig. 2.

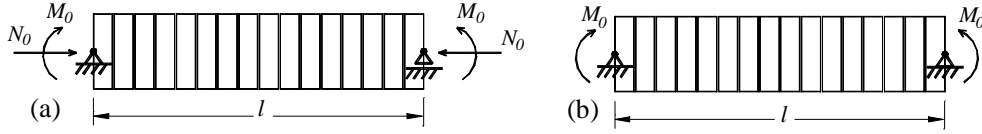


**Fig. 3.** Straight lintel (a) with no redundancy; (b) one time redundant.

The linear extension  $x$  of the compressed part of the section and of its plastic part  $y$  can be assumed as unknowns of the problem. According to Castigliano's method, let assume that the  $k^{\text{th}}$  approximation of the solution is known,  $x_k$  and  $y_k$  for which the corresponding axial thrust  $N_k^{EP}$  and moment  $M_k^{EP}$  and are deduced from eq.s (2); let assume that they are not able of equilibrating the current loading thrust  $N_k$  and moment  $M_k$  due to the opening of the joint and to its plastic response in compression. In order to avoid tensile stresses, the cross section height is updated and set equal to the current compressed part,  $h_{k+1} = x_k$ . Eq.s (3) represent, now, the only non equilibrated part of the external loads, due to the non linear material response; if we consider the elastic response of the section with updated height, these non equilibrated forces can be considered *fictitious external loads* to be added to the external ones. The procedure is summarized in the following.

- 1) Say  $N_0$  and  $M_0$  the external loads.
- 2) The  $k^{\text{th}}$  approximation of the solution is known:  $x_k, y_k$ , for which eq.s (3) show that the external loads are still unbalanced by an amount  $\Delta N_k^{EP}$  for the axial thrust and  $\Delta M_k^{EP}$  on the bending moment.
- 3) The geometry of the section is updated to the effective height:  $h_{k+1} = x_k$  and the section is considered linear elastic.
- 4) The unbalanced forces  $\Delta N_k^{EP}$  and  $\Delta M_k^{EP}$  are added to the external loads:  $N_{k+1} = N_0 + \Delta N_k^{EP}$ ,  $M_{k+1} = M_0 + \Delta M_k^{EP}$ ; the updated loads are applied to the new geometry so that from the elastic response the new approximation  $x_{k+1}, y_{k+1}$  to the solution is obtained.
- 5) Convergence is met according to a criterion referring to the unbalanced part of the axial thrust:

$$\max \left\{ \frac{\Delta N_{EP}^{k+1} - \Delta N_{EP}^k}{N_{EP}^k}, \frac{\Delta M_{EP}^{k+1} - \Delta M_{EP}^k}{M_{EP}^k} \right\} \leq \varepsilon \quad (4)$$

where  $\varepsilon$  is the accepted tolerance.

The starting solution  $h_0, x_0$  and  $y_0$  is the elastic response of the structure in its initial full geometry to the applied external loads only.

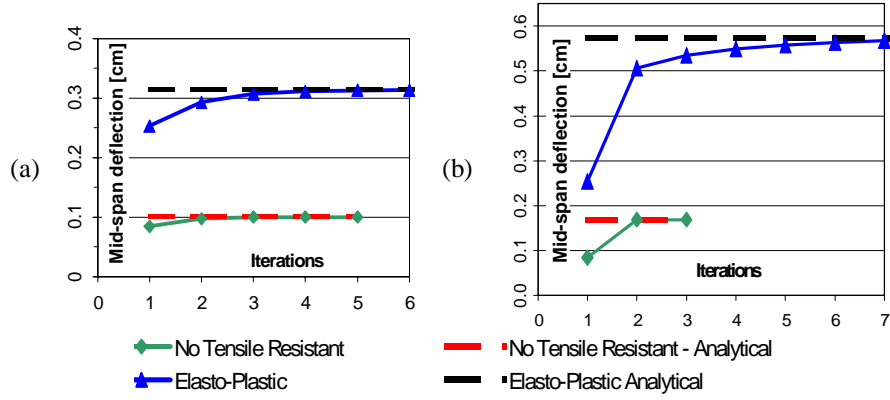


**Fig. 4.** Convergence of the procedure for a) isostatic and b) redundant straight lintel

In the example of Fig. 3 the external loads are constant being the problem non linear only in the material response. It can be proved that the procedure is convergent to the exact solution:

$$\lim_{k \rightarrow +\infty} (N_k^{EP} - N_0) = 0 \quad \text{and} \quad \lim_{k \rightarrow +\infty} (M_k^{EP} - M_0) = 0 \quad (5)$$

The outlined procedure is suitable for applications also on redundant structures, such as that of Fig. 3.b. Fig. 4 shows the convergence of the algorithm to the exact solution as a function of the number of iterations for both the isostatic and hyperstatic lintel in both the cases of elastic–No Tensile Resistant interfaces (Castigliano’s model) and elastic-plastic–No Tensile Resistant model herein proposed.

### SINGLE ARCH ELASTO-PLASTIC RESPONSE

The extension of Castigliano’s method presented in the previous section is essentially a mechanical model for the mortar joint. Therefore, it can be applied to generic structures also if the relation among axial thrust, bending moment, material properties and geometry is not known explicitly as in the straight lintel of Fig. 3.b. The procedure can be applied to generic structures following a predictor/corrector iterative scheme.

1. The  $(k-1)^{th}$  approximation of the solution is known, i.e. for each  $i^{th}$  section the height  $h_{k-1}^{(i)}$ , its compressed part  $x_{k-1}^{(i)}$ , the plastic plateau  $y_{k-1}^{(i)}$  and the external loads  $F_k^{(i)}$  to be applied in the next step are known.

2. *Prediction.* The geometry is updated so as to reduce the section height to the estimated compressed part:  $h_k^{(i)} = x_{k-1}^{(i)}$ . The external loads  $F_k^{(i)}$  are applied to the updated geometry for which the linear elastic response is computed; in particular the strain and displacement states are calculated.

3. *Correction.* On the basis of the strain and displacement states of each section, the compressed part  $x_k^{(i)}$ , the plastic plateau  $y_k^{(i)}$  and the unbalanced part of the internal forces  $\Delta N_k^{EP(i)}$  and  $\Delta M_k^{EP(i)}$  are computed via eq.s (3); it is worthwhile noting that the unbalanced forces are computed as a function of the current strain state only. Assuming  $\Delta N_k^{EP(i)}$  and  $\Delta M_k^{EP(i)}$  as the external fictitious forces representing the plastic response of

the material to be applied on every section in addition to the external loads, the loads are updated:  $\mathbf{F}_{k+1} = \mathbf{F}_0 + \Delta\mathbf{F}_k$ , where  $\Delta\mathbf{F}_k$  stands for a vector containing the whole of the fictitious forces.

4. The starting step is given by the elastic response to the external loads of the structure in its full geometry.

In the generic case of a redundant structure, the internal forces to be equilibrated are not known, like in the problem of a straight lintel, so that the convergence criterion cannot be referred to the unbalanced part of the external loads but is rather referred to the variation of the plastic fictitious forces between two subsequent steps:

$$\max \left\{ \left( \frac{\Delta N_{EP}^{k+1} - \Delta N_{EP}^k}{N_{EP}^k} \right)_i, \left( \frac{\Delta M_{EP}^{k+1} - \Delta M_{EP}^k}{M_{EP}^k} \right)_i, \forall i \right\} \leq \varepsilon \quad (6)$$

where the subscript  $i$  stands for the generic mortar joint, and  $\varepsilon$  is the accepted tolerance.

The procedure can be implemented by external programming of commercial F.E. codes since it is based on a series of elastic analysis of structures differing only because of an updating geometry and varying external fictitious forces. In particular, cfr. Fig. 1, an arch-type structure can be divided in finite beam-type elements in such a way that each element can represent a single arch block or brick. In this way:

1. the average axial thrust and bending moment in every element can be computed by averaging the nodal forces;
2. the strain and displacement states in the joints can be deduced from the averaged forces by means of the classical elastic beam theory,
3. the proposed procedure can be implemented by standard external programming of the F.E. code.

Since the proposed procedure can be regarded as a constitutive model for masonry rather than a mechanical model for mortar joints only, the finite elements discretizing the arch structure do not need to preserve the voussoir's dimension. They can represent an assemblage of bricks introducing the approximation that the elasto-plastic response is not allowed in every joint but, say, every  $n$  joints.

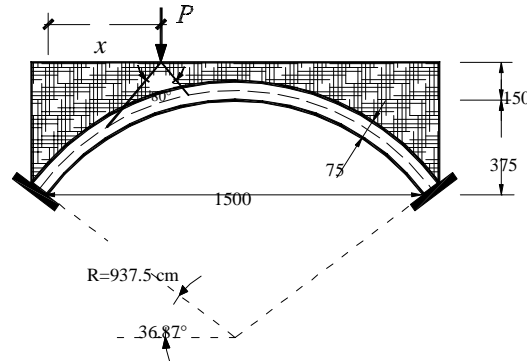


**Fig. 5.** Flat arch geometry. The shaded area represents the fill.

**Table 1.** Geometric and mechanical properties of the bridge

Property	Value	Property	Value
Span (intrados) $s$ [cm]	1500	Width (unity) [cm]	100
Rise (intrados) $r$ [cm]	375	Rise to Span ratio $r/s$	1/4
Ring thickness $d$ [cm]	75	Ring thickness to Span ratio $d/s$	1/20
Depth of fill in crown $f$ [cm]	75	Fill in crown to Ring thickness ratio $f/d$	1/1
Pier height $h$ [cm]	750	Pier height to Pier thickness ratio $h/t$	3.4
Pier thickness $t$ [cm]	220	Pier thickness to Ring thickness ratio $t/d$	2.9
Arch density [kN/m <sup>3</sup> ]	22	Load distribution in the fill	40°+40°
Fill density [kN/m <sup>3</sup> ]	24.1	Loaded length	knife type
Masonry			
Young's modulus [MPa]	15000	Masonry compressive strength [MPa]	5 / 10 / 15 / ∞

In the following, the procedure is applied to a single arch in which the discretization allows the crack to open every two joints and is developed using the ANSYS 5.6 F.E. code. The geometry of the arch, shown in Fig. 5 and summarized in Table 1, and was chosen so as to represent a typical flat arch extrapolating the geometry of the scale models tested by Melbourne and Wagstaff (1995).

The procedure had been applied to the arch considering different positions for the load, located at 0.1, 0.2, 0.3, 0.4 and 0.5 times the intrados span from the abutment, and assuming for masonry, first, the Castigliano's model for which no limit to compressive stresses is set (No Tensile Resistant model), than assuming a limit compressive stress of 15, 10 and 5 MPa. The fill has been considered having two different effects: 1) a dead load on the arch; 2) distributing (40°) the applied load in a limited area of the barrel.

In Fig. 6 the deformed shape at collapse is shown for two loading positions, giving evidence to the extension and position of the plastic hinges. The collapse mechanism and hinge geometry is quite similar for all the arch models almost independently on the material compressive strength, so that the deformed shape of Fig. 6 can be assumed as representative of all the models.

Figs 7 and 8 represent the load-displacement response of the arch (the displacement is referred to the point just below the loading line). It can be clearly seen, Fig. 7, that the response is quasi independent on the masonry compressive strength when the load is nearby 1/4 of the arch span: in this case the collapse is the result of a collapse mechanism which activates at relatively low stress levels in the arch. When the load is located on the center line, the line of thrust tends to move outwards the arch at the very end of the loading process when compressive stresses are quite high: in this case the elasto-plastic response of masonry, i.e. of the mortar joints, is of great effect on the collapse load.



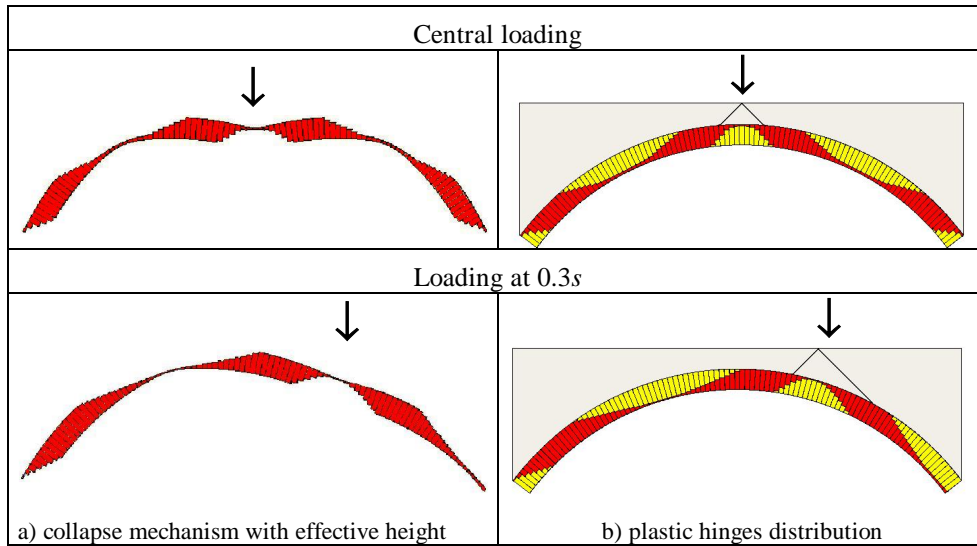


Fig. 6. a) collapse mechanism; b) plastic hinges– yellow areas are the open part of the joints.

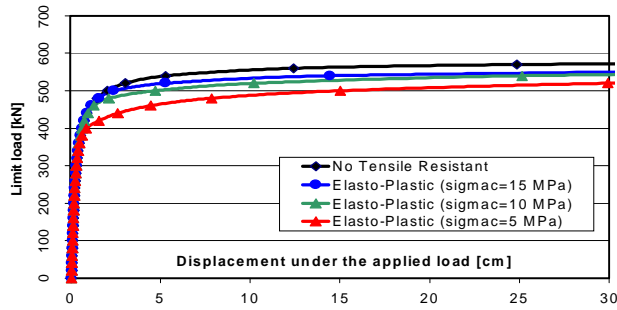


Fig. 7. Load-displacement response of the arch for load located at  $x/s = 0.3$ .

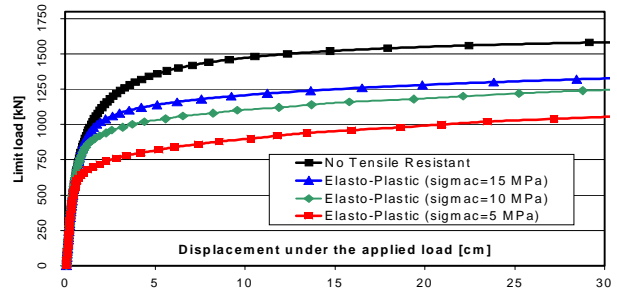


Fig. 8. Load-displacement response of the arch for central loading.

Fig. 9 plots the limit load of the four different models of the arch as a function of the load position. The most challenging position is located nearby 1/4 of the arch span, but specific numerical values account for  $x=0.3s$  as the position for which the arch exhibits the lowest limit load. For the considered geometry, the elasto-plastic response of the material turns out to have relevant effects on the limit load only for loads located nearby the center line.

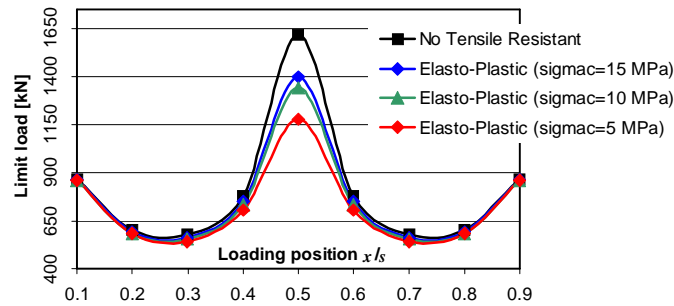


Fig. 9. Limit load of the arch vs. loading position and masonry strength.

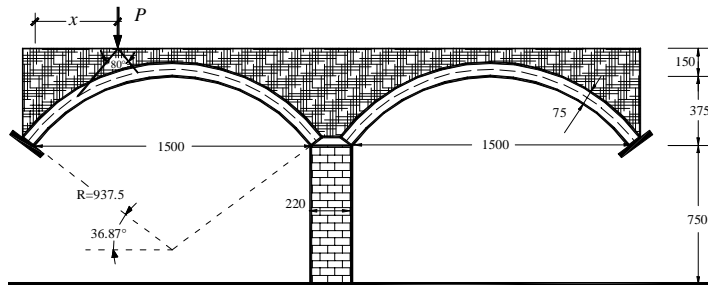


Fig. 10. Twin arch bridge geometry. The shaded area represents the fill.

### MULTI-SPAN ARCH BRIDGES ELASTO-PLASTIC RESPONSE

Figs 10 and 11 show the geometry of the considered twin- and three-span arch bridges which resemble that of the scale models tested by Melbourne and Wagstaff (1995) but for the ring thickness, which has been reduced to a more typical value.

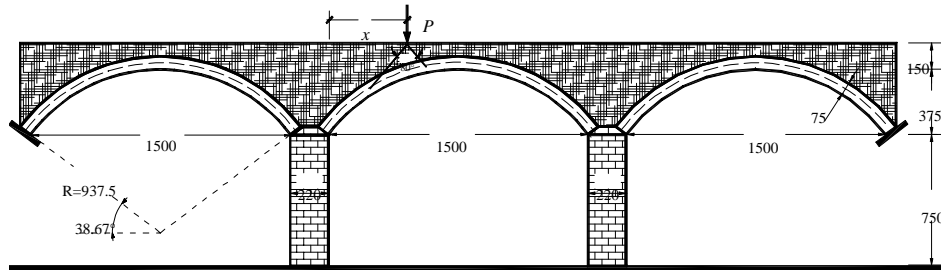
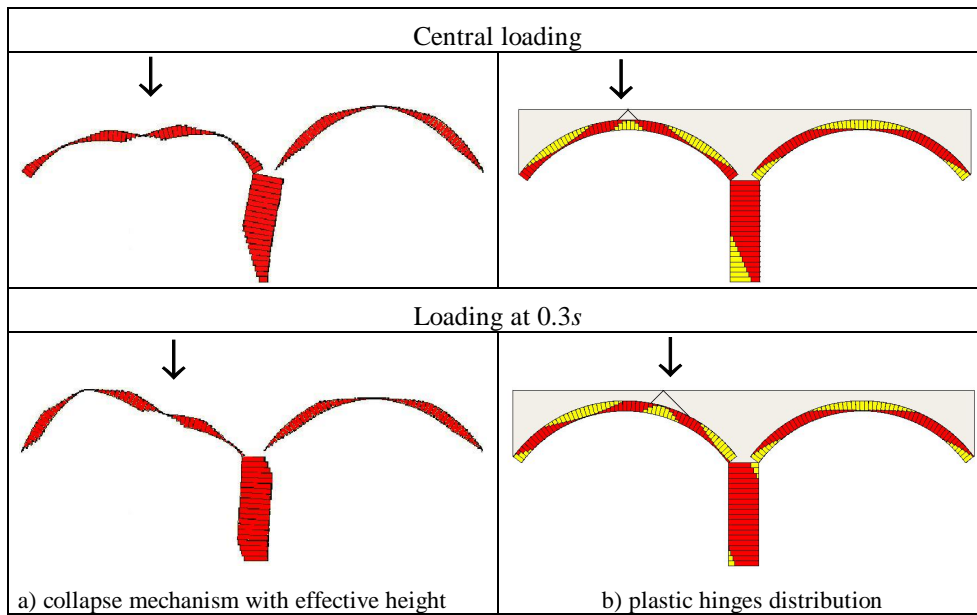
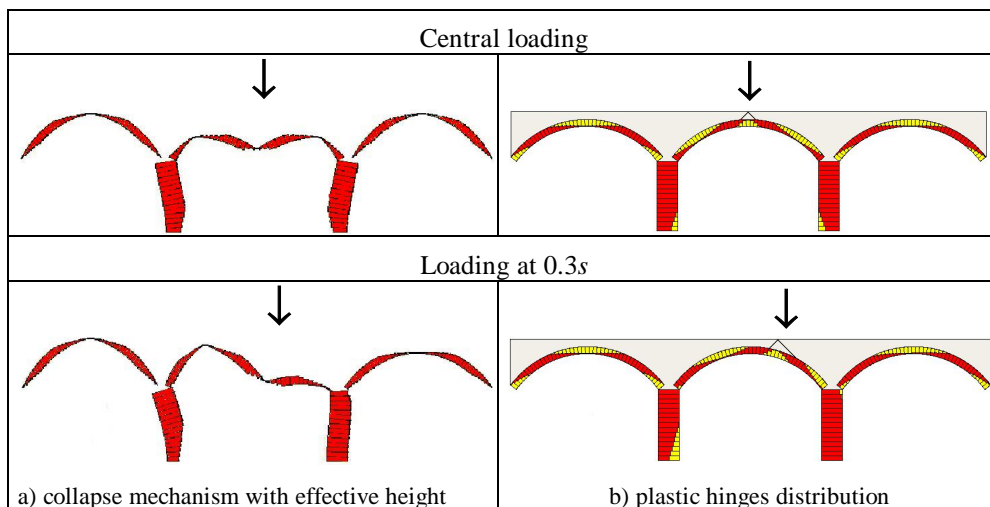


Fig. 11. Three-span arch bridge geometry. The shaded area represents the fill.

The same four different models for the single span arch (Castigliano's model, named No Tensile Resistant, models with compressive strength of 15, 10 and 5 MPa) have been developed for these two bridges, loading the arches up to collapse in different positions governed by the distance  $x$  from the abutment (see Figs 10 and 11). Figs 12 and 13 represent the collapse mechanisms for loading along the center line and at  $x = 0.3s$ , the same as for Fig. 6, pointing out the hinge geometry and location.



**Fig. 12.** a) collapse mechanism; b) plastic hinges – yellow areas are the open part of the joints.



**Fig. 13.** a) collapse mechanism; b) plastic hinges – yellow areas are the open parts of the joints.

Collapse mechanism involves 7 hinges for the twin arch model and 9 hinges for the three-arch one. The first results are coherent with Hughes (1995) on this kind of structures; the three-arch model response, instead, points out that the collapse mechanism involves all the three arches, as already conjectured by Melbourne and Wagstaff (1995) on the grounds of their experimental work. In particular, from the deformed shape of Fig. 13 it can be seen that, whatever the load position, the lateral arches are lifted upwards by the central arch, so that further applied load on the adjacent spans is likely to have stabilizing effects, as experimentally found by Melbourne and

Wagstaff (1995).

Plastic hinges with compressive stresses at the maximum threshold are found to activate at the last part of the load process. Their extension in space, involving quite large parts of the arch to develop, is a consequence of the mechanical model assumed of the mortar joint. The numbers near the plastic hinges refer to the progression of their formation.

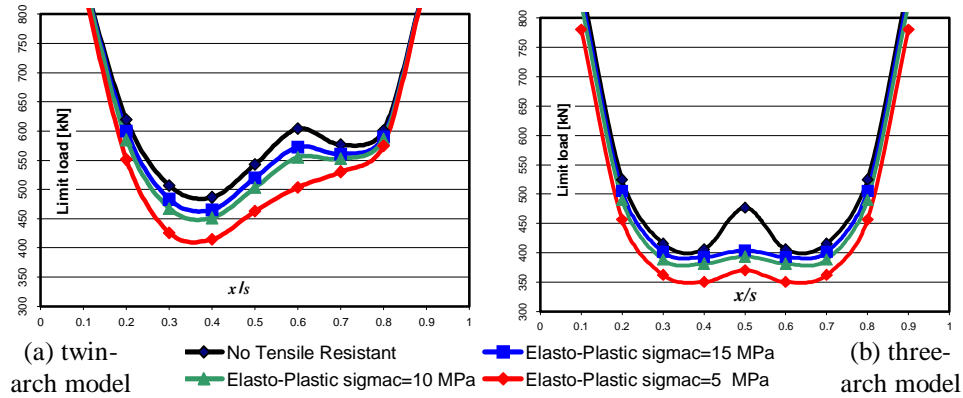


**Fig. 14.** Limit load of the twin-arch bridge vs. loading position and masonry strength.

Fig. 14 represents the limit load as a function of the load position and of the compressive strength for masonry. In the most dangerous positions, somewhere in-between  $0.25 \leq x/s \leq 0.75$ , the Castigliano's model (NTR) accounts for a limit load that is 15% to 20% for the twin arch model and 15% to 30% for the three-span bridge higher than the values predicted by the weakest, but realistic, elasto-plastic model.

## DISCUSSION

The effect of the arch ends compliances can be deduced from Fig. 15 where the limit load for the single-arch, twin- and three-arch models are plotted against the load position. The difference between the single-arch prevision and the calculated limit load for the real structure is sometimes dramatic: the single arch analysis always overestimates the bridge limit load, sometimes it foresees a limit load twice or more the real collapse load. The effect of material strength and of the number of spans is summarized in Table 2.

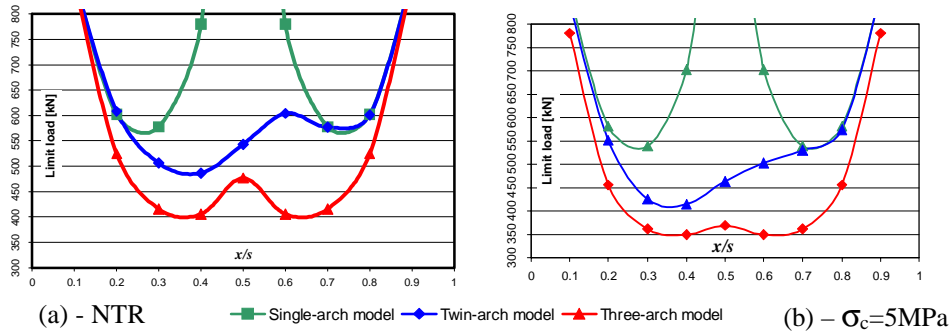


**Fig. 15.** Limit loads for the single-, twin- and three-span models vs. loading position for masonry) with a) unlimited compressive strength (NTR model); b) compressive strength of 5 MPa.

The effect of abutment compliance on the limit load had been studied by Falconer (1994) referring to a three-arch multi-span bridge and Hughes (1995) analyzing a twin-arch multi-span model. Falconer gives a reduction factor to account for abutment compliance as a function of the pier height-to-thickness ratio, while Hughes suggests a reductive factor that depends on all the relevant geometric factors of the bridge; for the specific values of the studied geometry, the two approaches foresee an overestimation of the single-arch analysis vs. the real limit load of 35% for the first estimate and 2% (knife type load) and 12% (for a 0.6m wide load footing); the classical MEXE (1968) method would suggest an overestimation of the single-arch analysis of 0% to 25%.

**Table 2.** Single-arch vs. multi-span analysis

NTR	$x/s=$	0.2	0.3	0.4	0.5	0.6	0.7	0.8
1-arch /2-arch		0%	+15%	+62.5%	$\rightarrow\infty$	+30%	0%	0%
1-arch /3-arch		+14%	+41%	+95%	$\rightarrow\infty$	+95%	+41%	+14%
$\sigma_c=5\text{MPa}$	$x/s=$	0.2	0.3	0.4	0.5	0.6	0.7	0.8
1-arch /2-arch		+5%	+29%	+70%	$\rightarrow\infty$	+40%	$\approx 0\%$	0%
1-arch /3-arch		+26%	+50%	+100%	$\rightarrow\infty$	+100%	+50%	+26%

The difference between the different estimates is quite unusual since Hughes' approach usually estimates reduction factors significantly higher than Falconer's one. In this specific geometry, the limit load for the isolated arch with perfectly built-in ends for central or near-central loading is quite high because the line of thrust hardly exits the arch thickness. A higher ring thickness, say 1 m, would lead to infinite collapse load for an NTR model because would allow two compressed spars to form inside the ring thickness and to directly support the external load, Fig. 16. In this case no reductive factor can be applied to the single-arch analysis and this is probably why estimates by Falconer, Hughes and the MEXE method are quite unreliable.

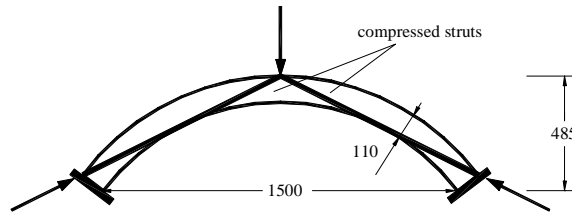


**Fig. 16.** Resistant mechanism in a thick flat arch.

## CONCLUSION

In this paper an iterative procedure for the elasto-plastic analysis of masonry arch structures has been discussed. The procedure proved to be efficient since it can be developed by simple external programming of commercial F.E. codes; besides, it allows the use of more sophisticated stress-strain relations in compression than the perfectly elasto-plastic model used in this work.

The comparison of the estimated collapse loads for single, twin and three-arch multi-span bridges showed that in some circumstances the classical single-arch approach dramatically overestimates the actual limit load. This happens when 1) the load is nearby the center of the span; 2) the material is poor with low compressive strength; 3) the ring thickness is high enough, in the single arch analysis, to make it possible for the thrust line to be straight and, nevertheless, entirely contained inside the arch thickness.

The analyses carried out on multi-span bridge models show that the estimates of the limit load for multiple arch bridges found in literature (BS 21/92, BA 16/93, 1993, Falconer, 1994, Hughes, 1995) seem to underestimate the effect of abutment compliance.

## ACKNOWLEDGMENTS

This research had been carried out by partial financial support of the National Earthquake Defense Group (GNDT) of the National Institute for Geophysics and Vulcanology (INGV) inside the VIA research project “*Seismic vulnerability reduction of infrastructural systems and environment*” (*Riduzione della vulnerabilità sismica di sistemi infrastrutturali e ambiente fisico*), a part of the Biennial 2000-2002 Research Program.

## REFERENCES

- Blasi, C., Foraboschi, P., (1994). Analytical approach to collapse mechanisms of circular masonry arches, *J. Struct. Engrg., ASCE*, **120**, 2288-2309.
- Boothby, T.E., (1997). Elastic plastic stability of jointed masonry arches, *Engng Str.s*, **19**, 345-351.
- Boothby, T.E., Domalik, D.E., Dalal, V.A., (1998). Service load response of masonry arch bridges, *J. Struct. Engrg*, **124**, 17-23.
- Bridle, R.J., Hughes, T.G., (1990). An energy method for arch bridge analysis, *Proc. Instn. Civ. Engrs.*, **89**, 375-385.

- Castigliano, C.A.P., (1879). *Theorie de l'équilibre des système elastique et ses application*, A.F. Negro ed., Torino.
- Choo, B. S., Coutie, M.G., Gong, N.G. (1991). Finite-Element analysis of masonry arch bridges using tapered elements, *Proc. Instn. Civ. Engrs.*, **91**, 755-770.
- Clemente, P., Occhiuzzi, A., Raithel, A., (1995). Limit behaviour of stone arch bridges, *J. Struct. Engrg.*, ASCE, **121**, 1045-1050.
- Como, M., (1998). Minimum and maximum thrusts states in Statics of ancient masonry bridges, *Proc. II Int. Arch Bridge Conf.*, A. Sinopoli ed., Balkema, Rotterdam, 321-330.
- Crisfield, M.A., (1985). Finite element and mechanism methods for the analysis of masonry and brickwork arches, *Transport and Road Research Laboratory, Dept. of Transport*, Research Report 19.
- Crisfield, M.A., Packham, A.J., (1988). A mechanism program for computing the strength of masonry arch bridges, *Transport and Road Research Laboratory, Dept. of Transport*, Research Report 124.
- Department of Transport, (1993.a). The assessment of highway bridges and structures, Department Standard BS 21/93.
- Department of Transport, (1993.b). The assessment of highway bridges and structures, Department Advice Note BA 16/93.
- Falconer, R.E., (1994). Assessment of multi-span arch bridges, *Proc. 3<sup>rd</sup> Int. Conf. on Inspection, Appraisal, Repair and Maintenance of Buildings and Structures*, Bangkok, 1994, 79-88.
- Gilbert, M., Melbourne, C., (1994). Rigid-block analysis of masonry structures, *The Str. Eng.*, **72**, 356-361.
- Harvey, W.E.J., (1988). Application of the mechanism analysis to masonry arches, *The Structural Engineer*, **66**, 77-84.
- Heyman, J., (1982). *The masonry arch*, Ellis Horwood, Chichester.
- Hughes, T.G., (1995). Analysis and assessment of twin-span masonry arch bridges, *Proc. Instn. Civ. Engrs.*, **110**, 373-382.
- Hughes, T.G., Blackler, M.J., (1997). A review of the UK masonry arch assessment methods, *Proc. Instn. Civ. Engrs.*, **122**, pp. 305-315.
- Loo, Y.C., Yang, Y., (1991). Cracking and failure analysis of masonry arch bridges, *J. Struct. Engrg.*, ASCE, **117**, 1641-1659.
- Lourenço, P.B., Rots, J.G., (2000). An anisotropic failure criterion for masonry suitable for numerical implementation, *Mas. Soc. J.nl*, **18**, 11-18.
- Melbourne, C., Wagstaff, W., (1993). Load tests to collapse of three large scale multispan brickwork arch bridges, *Bridge Management*, Harding ed., vol. 2, Thomas Telford, London.
- Melbourne, C., Gilbert, M., Wagstaff, W., (1995). The behaviour of multi-span arch bridges, *Proc. I Int. Arch Bridge Conf.*, C. Melbourne ed., Thomas Telford, London, 489-497.
- Military Engineering Experimental Establishment, (1963). Military Load Classification of Civil Bridges (Solog Study B.38), Christchurch, Hampshire.
- Molins, C. Roca, P., (1998.a). Capacity of masonry arches and spatial frames, *J. Str. Eng.rg*, **124**, 653-663.
- Molins, C. Roca, P., (1998.b). Load capacity of multi-arch masonry bridges, The behaviour of multi-span arch bridges, *Proc. II Int. Arch Bridge Conf.*, A. Sinopoli ed., Balkema, Rotterdam, 213-222.
- Ng, K.H., Fairfield, C.A., Sibbad, A., (1999). Finite-elament analysis of masonry arch bridges, *Proc. Instn. Civ. Engrs., Structs. & Bridgs.*, **134**, 119-127.
- Owen, D.R.J., Peric, D., Petrinic, N., Brookes, C.L., James, P.J., (1998). Finite/discrete element models for assessment and repair of masonry structures, *Proc. II Int. Conf. on Arch Bridges*,

- A. Sinopoli ed., 195-204, Balkema, Rotterdam.
- Page, J., (1987). Load test to collapse of masonry arch bridges at Preston, Shropshire and Prestwood, Staffordshire, *Department of Transport, TRRL Research Report 110*, Transport Research Laboratory, Crowthorne.
- Page, J., (1993). Masonry arch bridges. TRL - State of the art review, Department of Transport, HMSO, London.
- Pippard, A.J.S., Ashby, R.J., (1939). An experimental study of the voussoir arch, *Inst.n Civ. Eng.*, **10**, 383-403.
- Pippard, A.J.S., (1948). The approximate estimation of safe loads on masonry bridges, *Civil engineer in war*, **1**, 365, *Inst.n Civ. Eng.rs.*
- Ponniiah, D.A., Prentice, D.J., (1998). Load carrying capacity of masonry arch bridges estimated from multi-span model tests, *Proc. Instn. Civ. Engrs.*, **128**, 81-90.
- Rosson, B.T., Søyland, K., Boothby, T.E., (1998). Inelastic behaviour of sand-lime mortar joint masonry arches, *Eng.ng Str.s.*, **20**, 14-24.
- Royles, R., Hendry, A.W., (1991). Model tests on masonry arches, *Proc. Instn. Civ. Engrs.*, **91**, 299-321.
- Taylor, N., Mallinder, P., (1993). The brittle hinge in masonry arch mechanism, *The Struct. Eng.*, **71**, 359-366.